

NIST gold nanoparticle reference materials do not induce oxidative DNA damage

Bryant C. Nelson¹, Elijah J. Petersen¹, Bryce J. Marquis¹, Donald H. Atha¹, John T. Elliott¹, Danielle Cleveland¹, Stephanie S. Watson¹, I-Hsiang Tseng¹, Andrew Dillon², Mellisa Theodore³ & Joany Jackman³

¹National Institute of Standards and Technology, Material Measurement Laboratory, Gaithersburg, MD, USA, ²Department of Chemical Engineering, University of Maryland at Baltimore County, Baltimore, MD, USA and ³The Johns Hopkins University, Applied Physics Laboratory, Laurel, MD, USA

Abstract

One primary challenge in nanotoxicology studies is the lack of well-characterised nanoparticle reference materials which could be used as positive or negative nanoparticle controls. The National Institute of Standards and Technology (NIST) has developed three gold nanoparticle (AuNP) reference materials (10, 30 and 60 nm). The genotoxicity of these nanoparticles was tested using HepG2 cells and calf-thymus DNA. DNA damage was assessed based on the specific and sensitive measurement of four oxidatively-modified DNA lesions (8-hydroxy-2'-deoxyguanosine, 8-hydroxy-2'-deoxyadenosine, (5S)-8,5'-cyclo-2'-deoxyadenosine and (5R)-8,5'-cyclo-2'-deoxyadenosine) using liquid chromatography/tandem mass spectrometry. Significantly elevated, dose-dependent DNA damage was not detected at concentrations up to 0.2 µg/ml, and free radicals were not detected using electron paramagnetic resonance spectroscopy. These data suggest that the NIST AuNPs could potentially serve as suitable negative-control nanoparticle reference materials for *in vitro* and *in vivo* genotoxicity studies. NIST AuNPs thus hold substantial promise for improving the reproducibility and reliability of nanoparticle genotoxicity studies.

Keywords: DNA damage, genotoxicity, gold nanoparticles, mass spectrometry, reference materials

Introduction

There are many important unanswered questions regarding the environmental health and human safety risks posed by the widespread development and use of engineered nanoparticles (ENPs) (Nel et al. 2006). Currently, researchers cannot readily predict *a priori* the biological (Shaw et al. 2008) or toxicological (Oberdörster et al. 2005) effects of ENPs within a specified category (e.g. carbonaceous ENPs) or between categories (e.g. carbonaceous vs. metallic ENPs). For toxicological investigations in particular, ENP test results

should be both reproducible and comparable within and across test methods/laboratories in order for the results to be useful for risk assessment. Hence, there exists a practical need for well-characterised nanoparticle (NP) reference materials (RMs) and high-order reference methods for ENP toxicological studies (Aitken et al. 2008; Stone et al. 2009, 2010). Particularly important is the need for positive and negative control reference NPs that could be routinely used in such studies.

The National Institute of Standards and Technology (NIST) has developed three (10 nm, NIST RM 8011 - <https://www-s.nist.gov/srmors/reports/8011.pdf>; 30 nm, RM 8012 - <https://www-s.nist.gov/srmors/reports/8012.pdf>; 60 nm, RM 8013 - <https://www-s.nist.gov/srmors/reports/8013.pdf>) zero-valency state gold nanoparticle (AuNP) RMs that have been thoroughly characterised in terms of their physical and chemical properties and in terms of their sterility (endotoxins). Thus, these NPs hold promise for application as positive or negative NP controls in future nanotoxicology studies, but their toxicological effects need to be characterised.

A major mechanism of ENP toxicity arises from their potential to generate free radicals directly and/or to generate free radicals indirectly by altering or influencing intracellular signalling pathways (Nel et al. 2006). An overabundance of free radicals can damage biological molecules, such as DNA (for a thorough overview of ENP-induced DNA damage via free-radical mechanisms, the reader is referred to a recent review (Petersen & Nelson 2010)), inhibiting biological function. While macroscale gold (Au⁰) is generally considered to be chemically and biologically inert (Hammer & Norskov 1995), AuNPs have been shown to induce oxidative damage to DNA in cells (Grigg et al. 2009; Kang et al. 2009; Li et al. 2008). There have been many toxicological investigations on AuNPs focussing on cytotoxicity (Connor et al. 2005; Goodman et al. 2004; Jacobsen et al. 2009; Pan et al. 2009, 2007; Pernodet et al. 2006; Ponti et al. 2009; Shukla et al. 2005;

Tsoli et al. 2005), but fewer reports focussing specifically on genotoxicity (Grigg et al. 2009; Jacobsen et al. 2009; Kang et al. 2010, 2009; Li et al. 2008; Pfaller et al. 2010). In the DNA damage studies, AuNP-induced DNA damage was established by detecting and measuring increased levels of single strand breaks (via comet assay) in cellular DNA (Grigg et al. 2009; Kang et al. 2009; Singh et al. 2010) or by assessment of the accumulation of the 8-OH-dG lesion (via liquid chromatography with electrochemical detection) (Li et al. 2008) in DNA extracts. However, these studies typically dosed AuNPs at either very high solution concentrations ($\geq 20 \mu\text{g/mL}$), over a limited concentration range (Kang et al. 2009; Li et al. 2008), or at high AuNP flow rates in air ($\sim 27 \text{ nmol/cm}^2/\text{min}$) (Grigg et al. 2009). Mechanisms for AuNP-induction of DNA damage have not been definitively established in any of the reported studies, although Li et al. did demonstrate that DNA damage correlated with the down-regulation of specific DNA repair proteins (Li et al. 2008). The authors of this study suggested that AuNPs could be generating reactive oxygen species (ROS) that could potentially damage DNA, but evidence of this was not shown.

DNA damage evaluation using mass spectrometry (MS) allows one to quantitatively measure oxidative damage to individual DNA bases and elucidate the mechanisms of DNA damage induction based on the nature and quantity of lesions formed. MS approaches allow for measurement of oxidatively-induced DNA lesions such as 8-hydroxy-2'-deoxyguanosine (8-OH-dG); 8-hydroxy-2'-deoxyadenosine (8-OH-dA); (5S)-8,5'-cyclo-2'-deoxyadenosine (S-cdA); and (5R)-8,5'-cyclo-2'-deoxyadenosine (R-cdA) (Figure 1). The detailed mechanisms of oxidative DNA lesion formation have been comprehensively reviewed elsewhere (Dizdaroglu et al. 2002; Jaruga & Dizdaroglu 2008) but, in general, direct hydroxyl radical ($\cdot\text{OH}$) attack on DNA is the required initial step. In terms of biological relevance, 8-OH-dG is significant because of its known mutagenic and promutagenic activity, as it can cause $\text{G} \rightarrow \text{T}$ transversion mutations that are found in dysfunctional genes associated with cancer (Greenberg et al. 2001). Accumulation of 8-OH-dA in DNA causes $\text{A} \rightarrow \text{G}$ and $\text{A} \rightarrow \text{C}$ mutations, although 8-OH-dA has a lower mutation frequency in comparison to 8-OH-dG (Kamiya et al. 1995). The cdA lesions are unique in that they represent concomitant oxidative damage to both the sugar and base moieties of the same nucleoside. The 8,5'-cyclisation (for both the R and S diastereomers) causes distinct puckering of the sugar moiety giving rise to significant distortion in the DNA double helix (Jaruga & Dizdaroglu 2008). Accumulation of the S-cdA lesion has been shown to block DNA transcription, inhibit gene expression and induce transcriptional mutagenesis (Jaruga & Dizdaroglu 2008).

The present report describes the results from an *in vitro* genotoxicity study using the NIST AuNPs. The AuNPs were evaluated for their potential to induce oxidative damage to DNA in HepG2 cells. To more fully elucidate the mechanism for AuNP genotoxicity, AuNPs were also exposed to calf thymus DNA (ct-DNA), and their potential to cause free radicals was measured using electron paramagnetic resonance (EPR) spectroscopy. DNA damage was assessed based

on the specific detection and sensitive measurement of four modified 2'-deoxynucleosides lesions (8-OH-dG, 8-OH-dA, S-cdA and R-cdA) using isotope-dilution liquid chromatography/tandem mass spectrometry (LC/MS/MS). To our knowledge, this is the first application of MS for the quantitative evaluation of ENP-induced DNA modifications. Thus, this study was intended to carefully: (1) determine the mechanism of AuNP-induced oxidative DNA damage if damage is observed, (2) demonstrate the applicability of MS based methods to measure oxidatively-induced DNA damage after ENP exposure and (3) investigate the potential for NIST AuNPs to function as a positive or negative NP control for future nanotoxicology studies to help improve reproducibility and reliability of results.

Materials and methods

Reagents and materials

Nuclease P1, snake venom phosphodiesterase and alkaline phosphatase were purchased from US Biological (Swampscott, MA), Sigma-Aldrich (St. Louis, MO) and Roche Applied Science (Indianapolis, IN), respectively, in the United States. Stable-isotope labelled internal standards (ISTDs), R-cdA- $^{15}\text{N}_5$, S-cdA- $^{15}\text{N}_5$ and 8-OH-dA- $^{15}\text{N}_5$, were prepared using dATP- $^{15}\text{N}_5$ as previously described (Birincioglu et al. 2003). The 8-OH-dG- $^{15}\text{N}_5$ ISTD was custom synthesised by Cambridge Isotope Laboratories (Cambridge, MA, USA). All other chemicals and materials were obtained from Sigma-Aldrich and used as received, unless noted otherwise.

NIST AuNP reference materials

The 10, 30 and 60 nm citrate-stabilised AuNP RM solutions were obtained from the NIST Standard Reference Materials Program (RM 8011 <https://www-s.nist.gov/srmors/reports/8011.pdf>, RM 8012 <https://www-s.nist.gov/srmors/reports/8012.pdf> and RM 8013 <https://www-s.nist.gov/srmors/reports/8013.pdf>) and either utilised as received or diluted with distilled and deionised water (ddH_2O) and utilised as diluted solutions. The AuNP concentrations described in all experimental procedures are based on the concentration of gold atoms.

Experimental design

A number of related experiments were conducted to test the genotoxicity of NIST AuNPs and the mechanisms of the observed responses. HepG2 cells, a human liver carcinoma cell line, were chosen because this cell line has been widely used as a model to identify genotoxins (Knasmuller et al. 2004) and this cell line was used in a recent genotoxicity study with AuNPs (Singh et al. 2010). In contrast to most of the recent studies on AuNP genotoxicity, we chose to expose the HepG2 cells to AuNP doses $\leq 0.2 \mu\text{g/mL}$ to more closely approximate circulating levels of Au that are actually stored in tissues, i.e., mouse tissues after exposure to AuNPs (Niidome et al. 2006). While it is nearly always possible to obtain toxic responses at sufficiently high concentrations, the selected AuNP concentration range in the present study attempted to cover solely the biomedically relevant range. Moreover, the initial concentration of the NIST AuNPs was

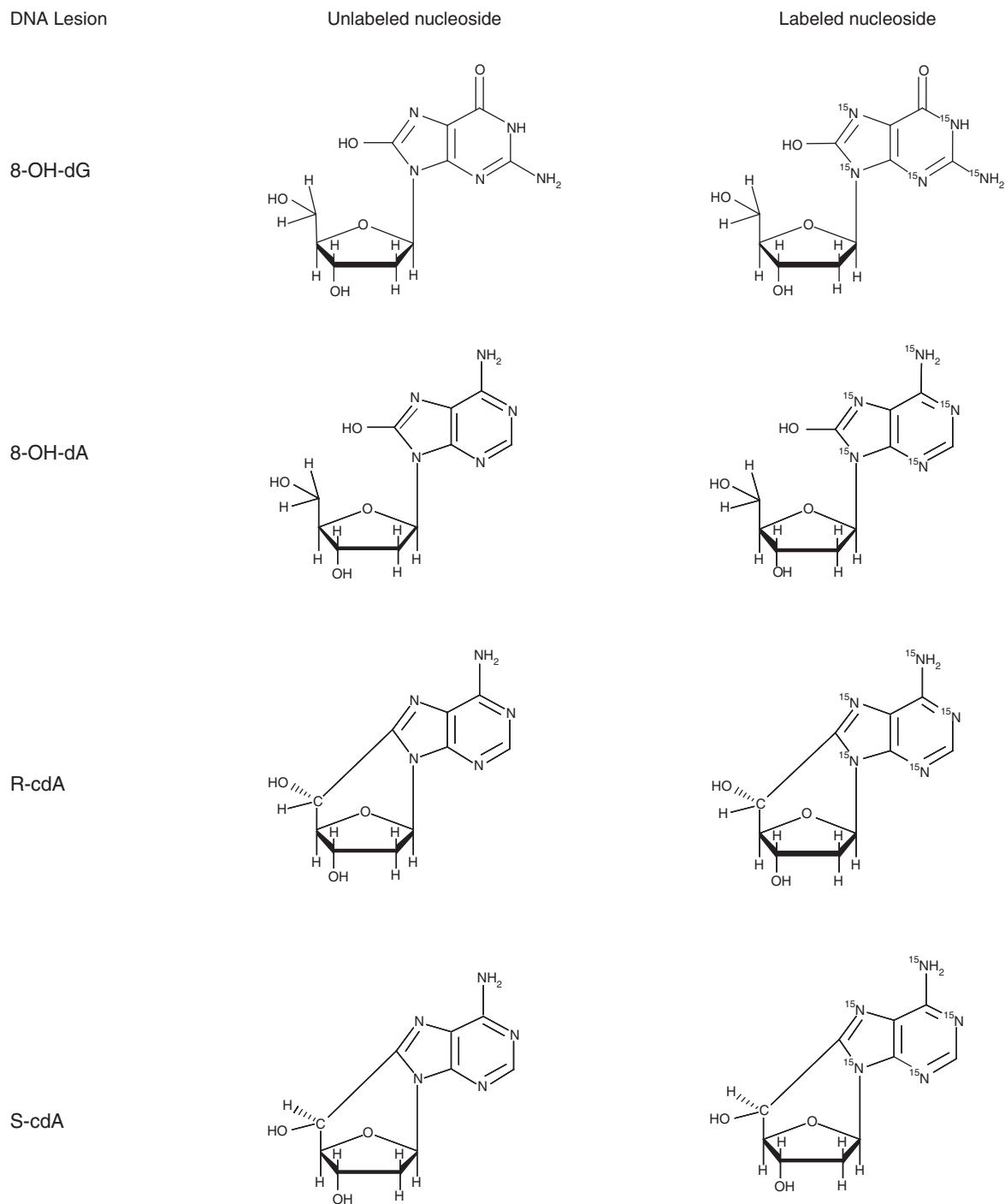


Figure 1. Chemical structures of the oxidatively-induced DNA lesions. Structures are shown for the unlabelled and stable-isotope labelled versions of each lesion.

50 $\mu\text{g}/\text{mL}$, and thus testing substantially higher concentrations would not be economically feasible and would likely require substantial manipulation of the AuNPs to concentrate them prior to their addition to the cell culture media. These manipulations would likely induce significant changes in the chemical and physical properties of the AuNP RMs. In our study, the ability of the AuNPs to enter the HepG2 cells was first investigated using transmission electron microscopy (TEM), a necessary step for most mechanisms of NP-induced DNA damage. Additionally, the cytotoxicity of these NPs was tested using the reduction of yellow

3-(4,5-dimethylthiazol-2-yl)-2,5-diphenyl tetrazolium bromide by mitochondrial succinate dehydrogenase (MTT assay) and a live/dead assay, and flow cytometry was used to assess if the NPs influenced the cell cycle (see the online supplementary material for details about the experimental methods for these assays). The lack of a toxic effect measured by these assays confirmed that any observed oxidatively-induced DNA damage was not a by-product of cell death and damage to DNA from lysed cells, a critical consideration when attempting to determine the mechanism of DNA damage (Petersen & Nelson 2010). In addition to

testing oxidatively-induced DNA damage using HepG2 cells exposed to AuNPs, the potential and mechanism for AuNPs to cause DNA damage was more fully investigated by measuring the capacity for AuNPs to produce free radicals using EPR, and by testing DNA damage in calf-thymus DNA exposed to NPs.

TEM measurements

Sixteen to twenty-four hours prior to addition to cells, appropriately diluted AuNP RMs were pre-incubated (37°C, 5% CO₂) in culture media: RPMI 1640 media supplemented with 10% FBS. This step was implemented to passivate the NP surface with proteins to mimic actual NP exposure conditions in human models (Li et al. 2008). Exponentially growing HepG2 cells were then cultured with the pre-incubated AuNPs for 24 h at 37°C in the presence of 5% CO₂. The final concentration of AuNP in each culture was 2 µg/L; this higher concentration, in comparison to the toxicity experiments, was used to facilitate determination of the AuNP distribution within the cells. Experiments were conducted in triplicate using independent 60 mm culture dishes. After the appropriate incubation time with the AuNPs, the supernatant was removed from culture dishes, and the cells were washed with 5 mL of 1× PBS (Invitrogen). Cells were then fixed with 2% paraformaldehyde + 2.5% glutaraldehyde in 0.1 mol/L cacodylate buffer at room temperature for 30 min and then sectioned and stained. Images were acquired using a Philips BioTwin CM120 transmission electron microscope at The Johns Hopkins University Microscopy Facility.

Treatment of HepG2 cell cultures with AuNPs

Sixteen to twenty-four hours prior to addition to cells, appropriately diluted AuNP RMs were pre-incubated (37°C, 5% CO₂) in culture media. Exponentially growing HepG2 cells (ATCC) were then cultured with the pre-incubated AuNPs for 3 h at 37°C in the presence of 5% CO₂. The final concentration of AuNP in each culture was 0.0002, 0.002, 0.02 or 0.2 µg/mL; dynamic light scattering (DLS) measurements were taken for the AuNPs in cell media after 0, 4 h and 24 h to investigate NP aggregation as described in the online supplementary material. HepG2 cells were also cultured with pre-incubated AuNPs for 24 h to evaluate the effect of time on the accumulation of DNA lesions at the lowest (0.0002 µg/mL) and highest (0.2 µg/mL) AuNP concentrations only. Exposure of cells to 100 µmol/L hydrogen peroxide for 1 h was utilised as a positive control. All experiments were conducted in triplicate using independent T75 culture plates. At harvest, the supernatant was removed and cells were detached from each plate by first rinsing with Versene followed by incubation in 0.25% trypsin/EDTA. When cells showed signs of detachment, RPMI 1640 with FBS was added and cells were triturated thoroughly prior to being transferred to centrifuge tubes. Cells were pelleted at 1000 g for 5 min and washed twice using 1× PBS. Cells and cell extracts were kept on ice for all remaining procedures. Genomic DNA was extracted from cell pellets using QIAmp Genomic DNA extraction kit (Qiagen) according to the manufacturer's instructions. Eluted DNA was precipitated in a 1.5 mL Eppendorf tube using a solution of 1:2.5 (v/v) 5 mol/L ammonium

acetate and ice-cold absolute ethanol. After 20 min of cold incubation, the precipitate was pelleted at 18,000 g for 10 min and stored in absolute ethanol at -20°C. The DNA pellet was thoroughly washed three times with ice-cold 70% ethanol and once with ice-cold absolute ethanol. The absolute ethanol was removed from the pellet using a vacuum desiccator and the dry pellet was resolubilised (gentle horizontal shaking at 4°C) in 120 µL ddH₂O for 24 h. The concentration of the solubilised DNA was determined using ultraviolet-visible (UV-Vis) spectrophotometry. The required volume of DNA was transferred into a clean 1.5 mL Eppendorf tube so that the tube contained ~50 µg DNA. The four, oxidatively-modified nucleoside ISTDs were added to the tube, the sample was dried in a SpeedVac under vacuum and then stored at 4°C until enzyme digestion.

Treatment of ct-DNA with AuNPs

For preparation of test samples, 250 µL of a 500 µg/mL ct-DNA stock solution (prepared in ddH₂O) was added to a 1.5 mL Eppendorf tube and a specified volume of the appropriate AuNP RM solution + additional ddH₂O were added so that the final concentration of AuNP (gold atoms) in solution was 0.0002, 0.02 or 2 µg/mL. For preparation of control samples, all sample additions were identical except that ddH₂O was added in place of the AuNP RM solutions. All test and control samples were prepared in triplicate. Samples were subsequently incubated at 37°C for 4 h and then centrifuged at ~16,000 g for 60 min to pellet the AuNPs. The centrifugation procedure removed 98% of the AuNPs from the incubation solutions (determined via ICP-MS as described in the online supplementary material). Approximately 450 µL of the ct-DNA containing-supernatant was transferred into a 30 kDa molecular-weight-cutoff (MWCO) centrifugal filter unit (Millipore) and centrifuged at 7000 g for 15 min at 4°C. After washing the filter membrane with ddH₂O, the ct-DNA was reverse-eluted into a clean 1.5 mL Eppendorf tube and the concentration of the eluted ct-DNA was determined using UV-Vis spectrophotometry (1 absorbance unit = 50 µg DNA/mL at 260 nm). The required volume of ct-DNA was transferred into a clean 1.5 mL Eppendorf tube so that the tube contained 50 µg ct-DNA. The four ISTDs were added to the tube, the sample was dried in a SpeedVac under vacuum and then stored at 4°C until enzyme digestion.

Enzymatic digestion of DNA samples

DNA samples (50 µg) were dissolved in 50 µL of a 10 mmol/L Tris-HCl solution (pH 7.5) supplemented with 2.5 µL of 1 mol/L sodium acetate containing 45 mmol/L zinc chloride (pH 6.0). Samples were incubated with nuclease P1, phosphodiesterase I and alkaline phosphatase for 24 h at 37°C in a water bath as described previously (Jaruga et al. 2004). The hydrolysed samples were transferred into a 3 kDa MWCO centrifugal filter units (Millipore) and centrifuged at ~16,000 g (75 min, 4°C). The filtrates were transferred into glass autosampler vials and analysed by LC/MS/MS.

DNA damage measurements using LC/MS/MS

Two separate LC/MS/MS analyses were performed on each DNA sample: one analysis for the hydroxyl-adduct lesions

(8-OH-dG and 8-OH-dA) and one analysis for the tandem lesions (*R*-cdA and *S*-cdA) (Jaruga et al. 2009). The description of each LC/MS/MS method and the lesion analysis parameters for each method are provided in the online supplementary material.

EPR spectroscopy experiments

Incubation systems with and without ct-DNA (250 µg/mL) and each of the three AuNP RMs (10 µmol/L) were mixed with 3-amino-2, 2, 5, 5-tetramethyl-1-pyrrolidinyloxy (AP) spin-trap solution (100 µmol/L) for EPR measurement. A Bruker Elexsys E500 spectrometer equipped with an X-band microwave bridge was used to perform EPR spectroscopy. The concentration of AP, as well as the EPR instrument parameters, was optimised to obtain the appropriate signal intensity and sensitivity for the AuNP RM incubation systems. The following instrument parameters were used: microwave power = 10 mW, modulation frequency = 100 kHz and modulation amplitude = 0.1 mT. AuNP RM or AuNP RM/ct-DNA incubation solutions, with the addition of AP spin-trap solution, were incubated in a water bath (37°C, 1 h) before each EPR measurement to mimic AuNP RM/ct-DNA incubation conditions. The incubation/spin trap systems were measured for 30 min to ensure equilibrium. In addition, *in-situ* UV EPR experiments via irradiation of the cavity were performed after the 30 min measurements of the incubation/spin-trap system to determine AuNP reactivity by creation of free radicals using a 500 W Xe arc lamp.

Statistical analysis

Graphpad Prism 5.0 software was utilised for statistical analyses. Significant differences were determined by one-way analysis of variance with *post hoc* Dunnett's multiple comparison test ($\alpha = 0.05$) between the control samples and the experimental samples in terms of the measured lesion levels for all of the tested NPs across the investigated AuNP dose range.

Results

Evaluation of AuNP uptake

DLS measurements showed no evidence of NP aggregation in cell media during a 24 h period (online supplementary Table S1). TEM images confirmed that the AuNPs were taken up by the HepG2 cells during the experimental incubation procedures. A characteristic TEM image (Figure 2) of a cell taken from a 24 h, 30 nm AuNP incubation experiment shows the existence of single, non-aggregated AuNPs (dark clusters) dispersed throughout the cytoplasm. The NPs are located in endosomal/lysosomal vesicles but not in organelles, such as the nucleus. No AuNPs were present in control cells.

Influence of AuNPs on cell viability and cell cycle

Results from the MTT assay (Figure 1S) showed that the AuNPs had no statistically significant effect (compared to negative control samples) on the proliferation of HepG2 cells. Results from the live-dead assay (Figure 2S) showed that the AuNPs produced a small decrease (compared to negative control samples) in the percentage of live cells in HepG2 cell culture (based on fluorescence). The average

decrease in the percentage of live cells in culture (95% → 75%) was independent of AuNP size and dose level. Results from flow cytometry cell cycle analysis showed no statistically significant changes in the G₀-, G₁-, S-, G₂- or M-phases of the HepG2 cell cycle (compared to negative control samples) for all of the tested AuNP sizes and doses from 0 to 72 h (data not shown). Altogether, these three different measurements of cytotoxicity indicated a lack of toxic effects on the cells as a result of AuNP exposure for a range of exposure times and NP concentrations. Thus, any DNA damage observed in subsequent experiments can be attributed directly to genotoxic effects of the NPs themselves and not cell death.

AuNP-induced oxidative damage to DNA in HepG2 cells

The effect of the AuNPs on the generation of oxidatively-modified DNA lesions in HepG2 cells was assessed using isotope-dilution LC/MS/MS. Figure 3 shows the characteristic DNA damage results for the 30 nm AuNP, while online supplementary Figures 3S and 4S show the characteristic DNA damage results for the 10 and 60 nm AuNPs, respectively. The positive control, H₂O₂, generated significantly increased levels of 8-OH-dG and 8-OH-dA, but had no significant effect on the levels of *R*-cdA and *S*-cdA. The measured levels of these lesions are shown as magnified figure insets because the background levels of the tandem lesions are one to three orders of magnitude lower in abundance than 8-OH-dG and 8-OH-dA in the HepG2 cells. In general, there were few statistically significant differences in the measured lesion levels between control and experimental samples for the AuNPs across the investigated dose range. The two exceptions concerned the levels of *S*-cdA at the 0.0002 µg/mL dose. The 30 nm NPs produced a statistically significant increase in the measured level of *S*-cdA (compared to the control) when dosed at a level of 0.0002 µg/mL (Figure 3A), but the increase in the level of *S*-cdA was not dose-dependent (see Figures 3B, C, and D). Conversely, the 60 nm NPs produced a statistically significant decrease in the measured level of *S*-cdA (compared to the control) when dosed at a level of 0.0002 µg/mL (Figure 4SA), but the decrease in the level of *S*-cdA was also not dose-dependent (see Figure 4SB, 4SC and 4SD). Because of the lack of dose-response trend, it is likely that the isolated changes in the level of *S*-cdA are biologically insignificant. Unlike 8-OH-dG and 8-OH-dA, formation of *R*-cdA and *S*-cdA is inhibited by the presence of molecular oxygen, and thus it is unlikely that the observed changes in the *S*-cdA lesions represent artefacts from oxygen present in the buffers and solutions. Additionally, no significant differences from control lesion levels were observed for cells treated (0.0002 or 0.2 µg/mL AuNPs) with 10, 30 or 60 nm NPs for 24 h (data not shown).

AuNP-induced oxidative damage to ct-DNA

The effect of the AuNPs on the generation of oxidatively-modified DNA lesions in ct-DNA solutions after a 4 h incubation was also assessed using LC/MS/MS. Figure 4 shows the characteristic DNA damage results for the 30 nm AuNP, while online supplementary Figures 5S and 6S show the characteristic DNA damage results for the 10 and 60 nm AuNPs, respectively. Overall, there were no statistically significant

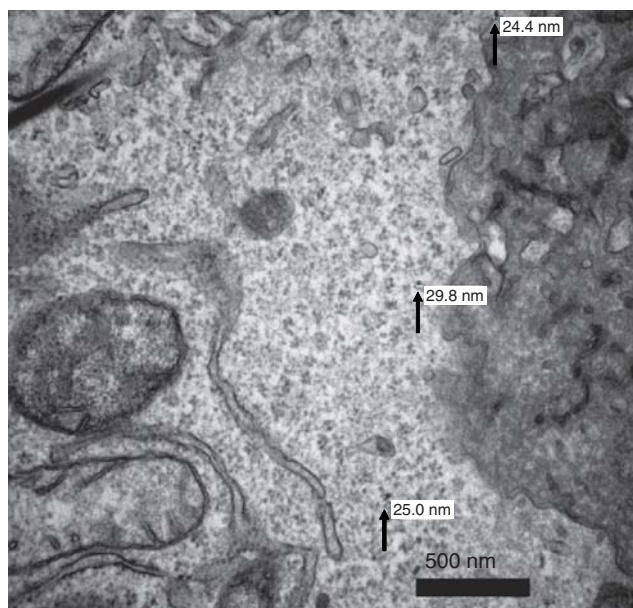


Figure 2. Morphology by TEM of a HepG2 cell incubated with 30 nm AuNPs. HepG2 cells were exposed for 24 h to 30 nm AuNPs (2 µg/mL), fixed with 2% paraformaldehyde + 2.5% glutaraldehyde in 0.1 mol/L cacodylate buffer, sectioned and visualised with a Philips BioTwin CM120 TEM. Image at 50,000× magnification of a representative cell with NPs subcellularly localised. AuNP, gold nanoparticle; NP, nanoparticle; TEM, transmission electron microscopy.

differences ($\alpha=0.05$) in the measured lesion levels between the control samples and the experimental samples for any of the tested NPs across the investigated AuNP dose range. The background level (control samples) of 8-OH-dG for the 60 nm NPs increased by a factor of almost two, in comparison to the background 8-OH-dG levels for the 10 and 30 nm NPs, a result most likely due to a sample preparation or sample storage artefact (Dizdaroglu 1998).

EPR spectroscopy of AuNP acellular incubation solutions

Free radical formation was not detected (the limit of detection for our EPR protocol was 0.332 µmol/L free radicals) in the AuNP incubation solutions (Figure 7SA and 7SB). The lack of free radical formation was independent of NP size, the presence or absence of ct-DNA or the input of high energy UV-irradiation.

Discussion

It is possible for NPs to directly enter the cell or even the nucleus and induce the formation of ROS (Auffan et al. 2009) which may then induce oxidative damage to DNA. In the present work, TEM analysis of the HepG2 cells demonstrated the uptake and the presence of monodisperse AuNPs in cytoplasmic vesicles scattered throughout the cytoplasm (see Figure 2 for an electron micrograph with 30 nm AuNPs). The presence of NPs as discrete spheres in vesicles is similar to a previous report demonstrating the rapid uptake of 18 nm citrate-stabilised AuNPs into human leukaemia cells (Connor et al. 2005). In this report, there was also no evidence for uptake of AuNPs into the nucleus. While some authors have found that AuNPs can induce double strand breaks if they target and enter the nucleus (Kang et al. 2010), other

investigators (Li et al. 2008) have shown that AuNPs do not have to enter the nucleus in order to induce oxidative damage to DNA.

In this study, biologically significant oxidative damage to genomic DNA was not detected in DNA extracted from HepG2 cells after exposure to a range of AuNP doses at relatively low concentrations (≤ 0.2 µg/mL) (Figures 3, 3S and 4S). This contrasts with previous findings which have shown significant DNA damage after AuNP exposure (Grigg et al. 2009; Kang et al. 2009; Li et al. 2008) but is in accordance with the study by Singh and co-workers (Singh et al. 2010). This may be a result of the lower concentrations used here in comparison to previous studies; Li et al. (2008) reported that AuNPs induced the formation of 8-OH-dG when the cells were dosed with AuNPs for 72 h at concentrations of 100 µg/mL, but not 50 µg/mL. Similarly, Singh and co-workers (Singh et al. 2010) found an increase, but not a statistically significant one, for glycolipid coated AuNPs at a concentration of 50 µg/mL compared to 5 µg/mL using HepG2 cells. Thus, there seems to be a threshold concentration below which AuNPs do not induce DNA damage.

The lack of DNA damage observed here in contrast to earlier studies may also partly stem from differences in the observed cellular distribution of the AuNPs, differences that may relate to characteristics of the cell lines utilised or of the NPs such as their surface coatings or size. For example, Kang et al. (2009) observed DNA damage using the comet assay for AuNPs that were 100 and 200 nm but not for those that were 4 and 15 nm. DNA damage was not observed here for particles that were 60 nm and smaller which suggests a potential AuNP size-dependent effect on DNA damage. However, DNA damage was observed previously using 20 nm (Li et al. 2008) and 8 nm particles (Grigg et al. 2009) but not 10 nm particles (Singh et al. 2010).

Another important difference between this and previous studies is the utilisation of isotope-dilution MS here which allowed us to quantify individual lesions, while the comet assay only provides a single, semi-quantitative measurement of DNA damage. A recent study by Pfaller et al. (2010) indicated that NP agglomerates can be observed in the comet tail during the comet assay which rendered even semi-quantification of DNA damage impossible. The extent to which this artefact may have impacted other studies using the comet assay is unclear, but apparent DNA damage was previously observed immediately after GeNP addition to cells (Lin et al. 2009), an artefact that could be explained by the presence of NP agglomerates in the DNA tail during the comet assay. Few studies have tested for this artefact by conducting the comet assay immediately after NP addition. MS based approaches for DNA lesion quantification offer an alternate analytical technique that avoids this potential artefact, while also offering numerous additional advantages such as quantitative results for multiple individual DNA lesions and the potential for mechanistic information from the lesion types and patterns.

Additional experiments using an acellular model and EPR were conducted to further investigate the reason for the apparent lack of oxidatively-induced DNA damage with HepG2 cells. Similarly to the cellular model results, the different AuNPs did not cause the formation of oxidatively-modified

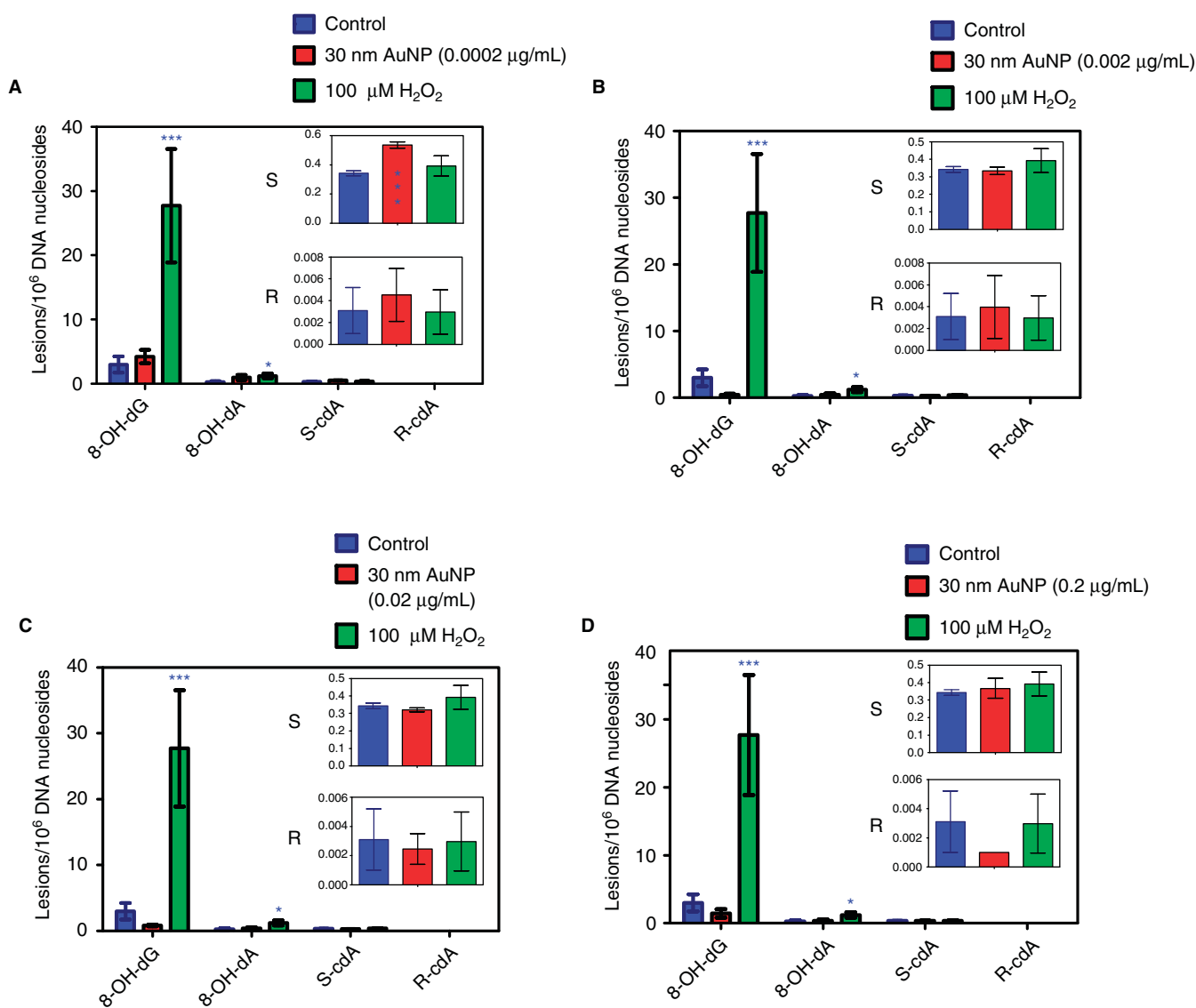


Figure 3. LC/MS/MS DNA damage evaluation of HepG2 cell cultures dosed with NIST 30 nm AuNP RMs. (A) Measured lesion levels in the presence of 0.0002 μg/mL AuNP. (B) Measured lesion levels in the presence of 0.002 μg/mL AuNP. (C) Measured lesion levels in the presence of 0.02 μg/mL AuNP. (D) Measured lesion levels in the presence of 0.2 μg/mL AuNP. Blue: control lesion level. Red: experimental lesion level. Green: positive control (H₂O₂) lesion level. The ratio of DNA lesions/10⁶ DNA nucleosides represents the mean from three independent samples. The error bars represent standard deviations. Statistical analyses based on one-way ANOVA with *post hoc* Dunnett's multiple comparison test: **p* Value < 0.05; ****p* Value < 0.001. ANOVA, one-way analysis of variance; AuNP, gold nanoparticle; LS/MS/MS, liquid chromatography/tandem mass spectrometry; NIST, National Institute of Standards and Technology; RM, reference material. S = ScdA, R = RcdA.

DNA lesions with ct-DNA (Figures 4, 5S and 6S). This suggests that the AuNPs would not have been likely to cause DNA lesions even if they had penetrated the nucleus. Complementary EPR spectroscopy experiments involving the incubation of AuNPs by themselves, in the presence of ct-DNA, and after *in situ* UV-irradiation showed that free radicals (hydroxyl radical or otherwise) were not generated (Figures 7SA and 7SB). These results raise questions about the potential for free radical formation caused by AuNPs to be a possible mechanism for DNA damage as postulated previously (Li et al. 2008). This result definitively confirms that these NPs would not directly produce free radicals in cytotoxicity assays and suggests that these AuNPs may also serve as a negative NP control for common cellular oxidative stress assays.

In summary, we have demonstrated that the citrate-stabilised AuNP RMs do not induce discrete, dose-dependent

oxidative damage to DNA in either HepG2 cells or ct-DNA at NP concentrations less than 0.2 or 2 μg/mL, respectively, nor do they cause cell death or produce free radicals. These results suggest that the AuNP RMs could potentially serve as suitable negative control materials for *in vitro* and *in vivo* genotoxicity studies that utilise DNA damage as the target endpoint. Additional research is thus necessary to confirm the lack of genotoxicity and cytotoxicity effects using a broader range of cell lines representative of the potential entry portals and/or target organs of the body. If the ability to use this RM as a negative control for a broad range of cells is established, the application of these NPs could substantially help increase the reliability of NP cytotoxicity investigations and help explain inter-laboratory discrepancies in nanotoxicity results.

Certain commercial equipment, instruments and materials are identified in order to specify experimental

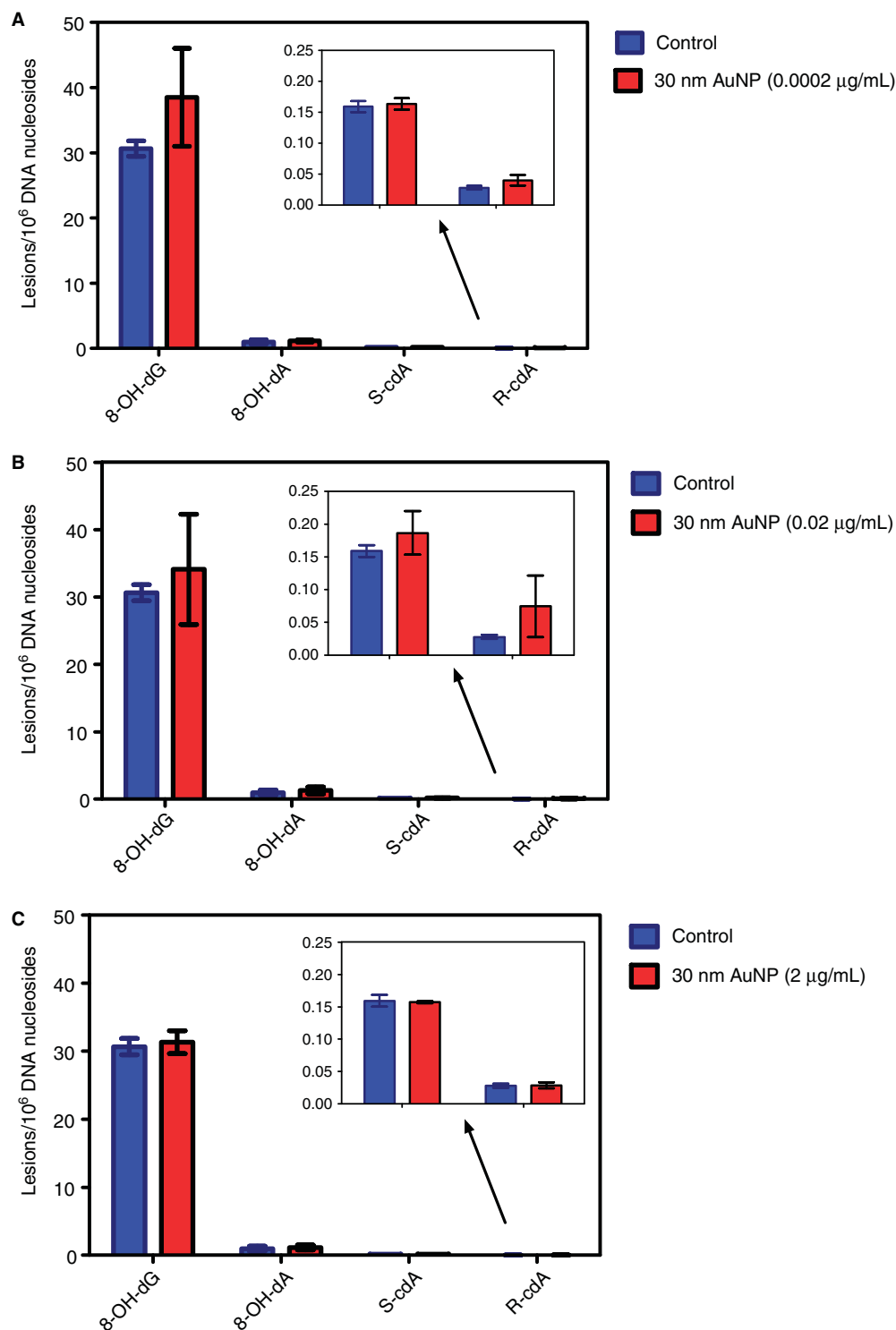


Figure 4. LC/MS/MS DNA damage evaluation of ct-DNA solutions dosed with NIST 30 nm AuNP RMs. (A) Measured lesion levels in the presence of 0.0002 $\mu\text{g/mL}$ AuNP. (B) Measured lesion levels in the presence of 0.02 $\mu\text{g/mL}$ AuNP. (C) Measured lesion levels in the presence of 2 $\mu\text{g/mL}$ AuNP. Blue: control lesion level. Red: experimental lesion level. The ratio of DNA lesions/ 10^6 DNA nucleosides represents the mean from three independent samples. The error bars represent standard deviations. Statistical analyses based on one-way ANOVA with *post hoc* Dunnett's multiple comparison test: ANOVA, one-way analysis of variance; AuNP, gold nanoparticle; ct-DNA, calf-thymus DNA; LS/MS/MS, liquid chromatography/tandem mass spectrometry; NIST, National Institute of Standards and Technology; RM, reference material.

procedures as completely as possible. In no case does such identification imply a recommendation or endorsement by the National Institute of Standards and Technology (NIST) nor does it imply that any of the materials, instruments or equipment identified are necessarily the best available for the purpose.

Acknowledgements

The authors acknowledge and thank Miral Dizdaroglu of NIST for his scientific advice and assistance with the DNA damage data interpretation. The authors would like to thank Teresa Butler, Vince Hackley, Stephen E. Long and Michael Winchester

of NIST for providing the AuNP RMs for the reported experiments and/or for helping to characterise the RMs in the calf-thymus DNA incubation samples. In addition, we would like to thank Alessandro Tona of NIST for culturing the HepG2 cells for the 24 h DNA damage portion of the study.

Declaration of interest

The authors report no conflicts of interest. The authors alone are responsible for the content and writing of the manuscript.

References

- Aitken RJ, Hankin SM, Tran CL, Donaldson K, Stone V, Cumpson P, et al. 2008. A multidisciplinary approach to the identification of reference materials for engineered nanoparticle toxicology. *Nanotoxicol* 2:71-78.
- Auffan M, Rose J, Orsiere T, Meo MD, Thill A, Zeyons O, et al. 2009. CeO₂ nanoparticles induce DNA damage towards human dermal fibroblasts *in vitro*. *Nanotoxicol* 3:161-171.
- Birincioglu M, Jaruga P, Chowdhury G, Rodriguez H, Dizdaroglu M, Gates KS. 2003. DNA base damage by the antitumor agent 3-amino-1,2,4-benzotriazine 1,4-dioxide (tirapazamine). *J Am Chem Soc* 125:11607-11615.
- Connor EE, Mwamuka J, Gole A, Murphy CJ, Wyatt MD. 2005. Gold nanoparticles are taken up by human cells but do not cause acute cytotoxicity. *Small* 1:325-327.
- Dizdaroglu M, Jaruga P, Birincioglu M, Rodriguez H. 2002. Free radical-induced damage to DNA: mechanisms and measurement. *Free Rad Bio Med* 32:1102-1115.
- Dizdaroglu M. 1998. Facts about the artifacts in the measurement of oxidative DNA base damage by gas chromatography mass spectrometry. *Free Rad Res* 29:551-563.
- Goodman CM, McCusker CD, Yilmaz T, Rotello VM. 2004. Toxicity of gold nanoparticles functionalized with cationic and anionic side chains. *Bioconjugate Chem* 15:897-900.
- Greenberg MM, Hantosi Z, Wiederholt CJ, Rithner CD. 2001. Studies on N⁴-(2-deoxy-D-pentofuranosyl)-4,6-diamino-5-formamidopyrimidine (Fapy dA) and N⁶-(2-deoxy-d-pentofuranosyl)-6-diamino-5-formamido-4-hydroxypyrimidine (Fapy dG). *Biochem* 40:15856-15861.
- Grigg J, Tellabati A, Rhead S, Almeida GM, Higgins JA, Bowman KJ, Jones GD, Howes PB, et al. 2009. DNA damage of macrophages at an air-tissue interface induced by metal nanoparticles. *Nanotoxicol* 3:348-345.
- Hammer B, Norskov JK. 1995. Why gold is the noblest of all the metals. *Nature* 376:238-240.
- Jacobsen NR, Moller P, Jensen KA, Vogel U, Ladefoged O, Loft S, Wallin H. 2009. Lung inflammation and genotoxicity following pulmonary exposure to nanoparticles in ApoE(-/-) mice. *Particle Fibre Toxicol* 6:2.
- Jaruga P, Dizdaroglu M. 2008. 8,5'-Cyclopurine-2'-deoxynucleosides in DNA: mechanisms of formation, measurement, repair and biological effects. *DNA Repair* 7:1413-1425.
- Jaruga P, Theruvathu J, Dizdaroglu M, Brooks PJ. 2004. Complete release of (5' S)-8,5'-cyclo-2'-deoxyadenosine from dinucleotides, oligodeoxynucleotides and DNA, and direct comparison of its levels in cellular DNA with other oxidatively induced DNA lesions. *Nucl Acids Res* 32:e87.
- Jaruga P, Xiao Y, Nelson BC, Dizdaroglu M. 2009. Measurement of (5'R)- and (5'S)-8,5'-cyclo-2'-deoxyadenosines in DNA *in vivo* by liquid chromatography/isotope-dilution tandem mass spectrometry. *Biochem Biophys Res Commun* 386:656-660.
- Kamiya H, Miura H, Murata-Kamiya N, Ishikawa H, Sakaguichi T, Inoue H, et al. 1995. 8-hydroxyadenine (7,8-dihydro-8-oxoadenine) induces misincorporation in *in vitro* DNA synthesis and mutations in NIH 3T3 cells. *Nucl Acids Res* 23:2893-2899.

- Kang B, Mackey MA, El-Sayed MA. 2010. Nuclear targeting of gold nanoparticles in cancer cells induces DNA damage, causing cytokinesis arrest and apoptosis. *J Am Chem Soc* 132:1517-1519.
- Kang JS, Yum YN, Kim JH, Song H, Jeong J, Lim YT, et al. 2009. Induction of DNA damage in L5178Y cells treated with gold nanoparticles. *Biomol Therapeut* 17:92-97.
- Knasmuller S, Mersch-Sundermann V, Kevekordes S, Darroudi F, Huber WW, Hoelzl C, et al. 2004. Use of human derived liver cell lines for the detection of environmental and dietary genotoxins; current state of knowledge. *Toxicol* 198:315-328.
- Li JJ, Zou L, Hartono D, Ong CN, Bay BH, Yung LYL. 2008. Gold nanoparticles induce oxidative damage in lung fibroblasts *in vitro*. *Adv Mat* 20:138-142.
- Lin MH, Hsu TS, Yang PM, Tsai MY, Perng TP, Lin LY. 2009. Comparison of organic and inorganic germanium compounds in cellular radiosensitivity and preparation of germanium nanoparticles as a radiosensitizer. *Int J Rad Biol* 85:214-226.
- Nel A, Xia T, Madler L, Li N. 2006. Toxic potential of materials at the nanolevel. *Science* 311:622-627.
- Niidome T, Yamagata M, Okamoto Y, Akiyama Y, Takahashi H, Kawano T, et al. 2006. PEG-modified gold nanorods with a stealth character for *in vivo* applications. *J Control Release* 114:343-347.
- Oberdorster G, Maynard A, Donaldson K, Castranova V, Fitzpatrick J, Ausman K, et al. 2005. Principles for characterizing the potential human health effects from exposure to nanomaterials: elements of a screening strategy. *Particle Fibre Toxicol* 2:1-35.
- Pan Y, Leifert A, Ruau D, Neuss S, Bornemann J, Schmid G, et al. 2009. Gold nanoparticles of diameter 1.4 nm trigger necrosis by oxidative stress and mitochondrial damage. *Small* 5:2067-2076.
- Pan Y, Neuss S, Leifert A, Fischler M, Wen F, Simon U, et al. 2007. Size-dependent cytotoxicity of gold nanoparticles. *Small* 3:1941-1949.
- Pernodet N, Fang X, Sun Y, Bakhtina A, Ramakrishnan A, Sokolov J, et al. 2006. Adverse effects of citrate/gold nanoparticles on human dermal fibroblasts. *Small* 2:766-773.
- Petersen EJ, Nelson BC. 2010. Mechanisms and measurements of nanomaterial-induced oxidative damage to DNA. *Anal Bioanal Chem* 398:613-650.
- Pfaller T, Colognato R, Nelissen I, Favilli F, Casals E, Ooms D, et al. 2010. The suitability of different cellular *in vitro* immunotoxicity and genotoxicity methods for the analysis of nanoparticle-induced events. *Nanotoxicol* 4:52-72.
- Ponti J, Sabbioni E, Munaro B, Broggi F, Marmorato P, Franchini F, et al. 2009. Genotoxicity and morphological transformation induced by cobalt nanoparticles and cobalt chloride: an *in vitro* study in Balb/3T3 mouse fibroblasts. *Mutagenesis* 24:439-445.
- Shaw SY, Westly EC, Pittet MJ, Subramanian A, Schreiber SL, Weissleder R. 2008. Perturbational profiling of nanomaterial biologic activity. *Proc Natl Acad Sci USA* 105:7387-7392.
- Shukla R, Bansal V, Chaudhary M, Basu A, Bhonde RR, Sastry M. 2005. Biocompatibility of gold nanoparticles and their endocytotic fate inside the cellular compartment: a microscopic overview. *Langmuir* 21:10644-10654.
- Singh S, D'Britto V, Prabhune AA, Ramana CV, Dhawan A, Prasad BLV. 2010. Cytotoxic and genotoxic assessment of glycolipid-reduced and -capped gold and silver nanoparticles. *New J Chem* 34:294-301.
- Stone V, Nowack B, Baun A, van den Brink N, von der Kammer F, Dusinska M, et al. 2010. Nanomaterials for environmental studies: classification, reference material issues, and strategies for physico-chemical characterisation. *Sci Total Environ* 408:1745-1754.
- Stone V, Johnston H, Schins RPF. 2009. Development of *in vitro* systems for nanotoxicology: methodological considerations. *Crit Rev Toxicol* 39:613-626.
- Tsoli M, Kuhn H, Brandau W, Esche H, Schmid G. 2005. Cellular uptake and toxicity of Au₅₅ clusters. *Small* 1:841-844.

Supplementary material available online

Supporting information including details on experimental methods to determine the toxicity of NIST gold nanoparticle reference materials are available online.